Simulation of a player–clarinet system

Scott D. Sommerfeldt and William J. Strong

Department of Physics and Astronomy, Brigham Young University, Provo, Utah 84602

A time-domain simulation model has been developed for investigating the player–clarinet system. The three components that constitute the simulation model consist of the player's air column, reed, and the clarinet. The player's air column is represented in terms of an analogous circuit model to obtain the mouth pressure. The reed is represented as a damped, driven, nonuniform bar. The clarinet is represented in terms of a scaled version of its input impedance impulse response. A convolution of the impulse response with the volume velocity determines the mouthpiece pressure. Use of the model is valid for both small- and large-amplitude reed oscillations. Many of the nonlinearities associated with the clarinet are incorporated in the model in a rather natural way. Several vocal tract configurations are investigated to determine the influence of the vocal tract on the player's air column impedance and the concomitant effect on the clarinet tone.

PACS numbers: 43.75.Ef

INTRODUCTION

Time-domain simulation of complex acoustical systems, such as the clarinet, can often be a powerful tool to supplement frequency-domain descriptions. This may be especially true when the system under study involves significant nonlinearities and when large amplitude and transient oscillations are studied. Ideally, a simulation model should match the actual physical system it represents as closely as possible in order to permit a study of subtle as well as gross functional behavior. We review briefly previous studies of the clarinet that generally have shown a progression from simpler to more complex models.

Backus (1963) was the first to develop a successful mathematical theory which described small oscillations in a clarinet. He assumed a constant blowing pressure at the mouthpiece, treated the reed as a damped, simple harmonic oscillator, and dealt with the case where the reed was driven by small-amplitude, sinusoidal oscillations of the air column. Backus was able to obtain a number of significant results, such as expressions for threshold blowing pressure, and frequency shift in the tone due to a phase shift in the reed vibrations relative to the mouthpiece pressure. Furthermore, he was able to obtain very good agreement between his theoretical and experimental results.

Benade and Gans (1968) were the first to investigate the nonlinear aspects of the clarinet. In their work, they developed a qualitative, nonlinear theory for oscillations in wind instruments. Later, Worman (1971) developed the mathematics to handle the nonlinear theory for the clarinet. He treated the reed as a damped, simple harmonic oscillator, as Backus had done, but he also considered nonlinear flow through the reed aperture. The nonlinear function describing flow was expanded in a power series, which was then truncated in order to keep the algebra tractable. Worman then used the truncated expansion to study a tube with one resonance and one antiresonance. With this model, he was able to obtain good agreement between theory and experiment. Schumacher (1978) developed a method that applied

an integral equation approach to Worman's equations. Schumacher's method, which did not suffer the limitations of truncation, was used to study a tube with three resonances and two antiresonances.

Only steady-state oscillations were studied in the work mentioned previously. In another study of the clarinet, Stewart and Strong (1980) treated the clarinet reed as a nonuniform bar clamped at one end, which seems to be a more realistic representation. They represented the clarinet simply as a straight cylindrical tube with no tone holes to which a tapered mouthpiece was attached. Schumacher (1981) applied the method of McIntyre and Woodhouse (McIntyre *et al.*, 1983) to study fairly realistic systems. Schumacher treated the reed as a simple harmonic oscillator and then developed an efficient method of calculating the convolution of the impulse response function with the volume velocity to obtain the mouthpiece pressure. The method represented significant improvement in calculation efficiency, and greatly enhanced the possibility of numerically studying a fairly realistic clarinetlike system. Transient and steady-state phenomena were simulated in both the Stewart and Schumacher studies.

In all the work mentioned previously, no consideration was given to the effect the player's air column might have. The player was simply represented by a constant pressure source. Mooney (1968) conducted an x-ray study in which he concluded that the shape of the vocal tract influenced the tonal spectrum of the clarinet. Clinch *et al.* (1982) published the results of a study in which the shape of the vocal tract was monitored with low-energy x-ray techniques. Using this approach, they studied the spectra of various clarinet and saxophone tones and concluded that the vocal tract resonance frequencies must be properly adjusted to obtain good tone production.

Benade and Hoekje (1982) and Benade (1983) studied the relationship of the input impedance of the player's air column to the reed impedance, the reed transconductance, and the clarinet impedance. They were able to demonstrate that the upstream impedance of the player's air column

should be important in tone production when it is comparable in magnitude to the downstream impedance of the instrument's air column. Benade (1983) reported player air column (PAC) impedance peaks of 500–750 Ω (cgs) with the vocal tract configured for /ɑ/, /ɛ/, or /ɪ/; clarinet impedance peaks of 350 Ω were reported. He also demonstrated an enhancement of the fourth harmonic of a clarinet tone when the PAC impedance was tuned to the frequency of the fourth harmonic of a clarinet tone.

Backus (1985) measured values of PAC impedance of less than 50 Ω which were an order of magnitude smaller than those of the clarinet ($\sim 800\ \Omega$). He was able to find only minimal effects of the vocal tract shape on the harmonic structure of clarinet tones. He observed larger changes when a more sharply tuned resonator was substituted for the PAC.

Hoekje (1986) measured PAC impedance values of about 50 Ω when the vocal tract was configured for /ɑ/ and values of about 300 Ω when the tract was /i/ configured. He measured a first mode impedance peak of about 650 Ω for a clarinet fingered for written C_4.

A precursor to the present study (Strong and Sommerfeldt, 1986; Sommerfeldt, 1986, Appendix A) was motivated by the results of a study of vowel production by Allen and Strong (1985) who studied the interaction of the subglottal system with the glottis and supraglottal system in vowel production. The glottis was represented using a parametrized glottal area function developed by Titze (1984). The supraglottal system was represented by its impulse response and the supraglottal pressure was calculated as the convolution of the impulse response with the glottal airflow. Allen and Strong found that there was significant interaction between the subglottal system, the glottis, and the supraglottal system.

In the present study, we have developed a time-domain simulation model and applied digital simulation techniques as a means of studying the effects of the PAC impedances on pressures and flow in a clarinetlike system. An effort has been made to incorporate several of the approaches discussed previously, thereby hoping to incorporate as many of the important features as possible, while still being able to deal with the model computationally. The model is valid for both small- and large-amplitude reed oscillations, and is capable of giving insight to questions concerning the vibration of the reed and damping due to the player's lip. The simulation incorporates a model of the PAC as well, so that questions regarding the influence of the PAC can be investigated. Waveforms and spectra have been obtained for the reed opening, the airflow through the reed opening, the mouth (PAC) pressure, and the tube (mouthpiece) pressure. Additionally, experimental results have been obtained for the reed opening and compared with the numerical results.

I. SIMULATION MODEL

In developing the model for the simulation, there were three different components comprising the system which we considered: the PAC (including the lungs, subglottal network, and vocal tract), the clarinet reed system, and the clarinet. In an attempt to model as realistically as possible, while still being able to efficiently obtain numerical results, we adapted several methods which had been previously developed by others.

The model for the PAC consisted of a series of 16 concatenated tubes, each 2.5 cm long. The vocal tract was represented with seven of these sections, whose cross-sectional area could be altered to give different tract configurations. The trachea and bronchi were represented as uniform tubes, the trachea being 12.5 cm in length, and the bronchi 5 cm in length. The equivalent cross-sectional areas of the two sections closest to the lungs were obtained from Ishizaka et al. (1976). The resistance of the lung network was represented as a lumped element resistance. Based on information from Ishizaka et al., a value of 4 Ω (cgs) was chosen as a reasonable estimate of the lung resistance.

To obtain numerical results, the PAC was treated as an analogous electric circuit (Flanagan, 1972). The equivalent circuit is given in Fig. 1, where

P_l = lung pressure,

$U_n(t)$ = volume velocity of nth section,

$UG_n(t)$ = volume velocity of nth loop containing compliance (C_n) and conductance (G_n),

$UA_n(t)$ = volume velocity of nth loop containing conductance (G_n) and wall admittance ($B_n M_n K_n$),
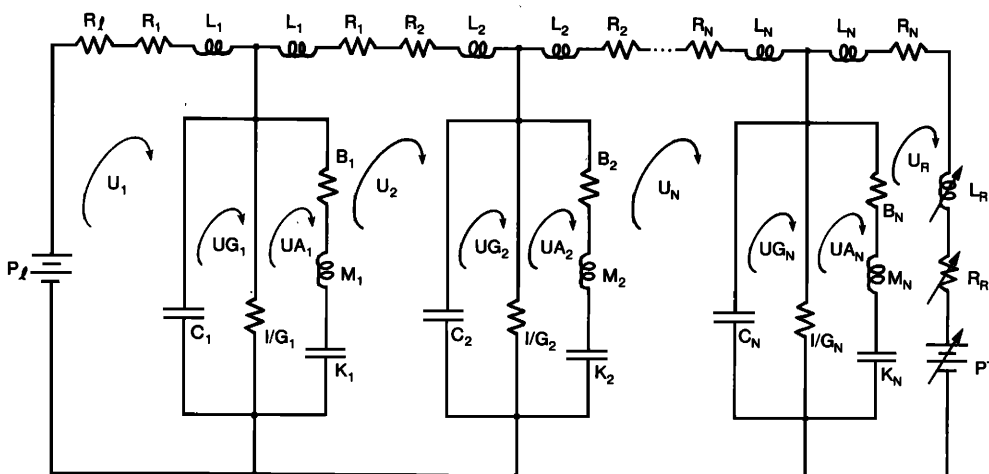

FIG. 1. Electrical circuit analog of the player's air column.

$R_R(t)$ = reed aperture resistance,

$L_R(t)$ = reed aperture inductance, and

$PT(t)$ = pressure in mouthpiece, to be described later.

The yielding walls of the PAC were modeled as a lumped element viscous-mass-compliance (BMK) circuit. Average values for B, M, and K were obtained from Ishizaka *et al.* (1975). Further details, including the governing equations, can be found in Appendix A. (We have used capital letter symbols to represent many of our time functions, in part because U is often used to represent volume velocity. There should be little reason for confusion with frequency functions that do not appear in explicit equation form.)

To solve the corresponding circuit equations on a computer, the integrals were represented as sums, and the derivatives as backward differences. The sampling frequency was set to 48 000 Hz, giving a sampling period of 21 μs. This value was chosen to ensure valid results in the frequency range of interest and to correspond to one of the standard audio sampling frequencies.

The reed was modeled as a damped, driven, nonuniform bar, based on the approach developed by Stewart and Strong (1980). Most often, the reed has been modeled as a simple harmonic oscillator, but a nonuniform bar model seemed more realistic and more capable of incorporating reed interactions with other parts of the system. In particular, the changes in effective reed mass and stiffness as the reed moves against the mouthpiece, the changing reed–lip interaction with reed position and the interaction of the reed with the air-stream are more naturally represented.

For transverse vibrations of a bar clamped at one end, the differential equation is given by Kinsler *et al.* (1982) as

$$\rho A \frac{\partial^2 y}{\partial t^2} = - YAK^2 \frac{\partial^4 y}{\partial x^4}, \tag{1}$$

where ρ is the mass density of the bar, A is its cross-sectional area, Y is its Young's modulus, K is its radius of gyration, and y is the transverse displacement. For a bar with rectangular cross section, $K = b/(12)^{1/2}$, where b is the bar thickness. If damping and a driving force are added, and account taken of the nonuniformity of the bar, the equation becomes

$$\rho A \frac{\partial^2 y}{\partial t^2} + R \frac{\partial y}{\partial t} = - \frac{\partial^2}{\partial x^2}\left(YAK^2 \frac{\partial^2 y}{\partial x^2} \right) + F, \tag{2}$$

where R is the damping per unit length, and F is the external applied force per unit length. The values of the constants used correspond to typical values for cane. For ρ, we used a value of 0.5 g/cm^3 and, for Y, we used a value of 6×10^{10} dyn/cm^2. It is not claimed that these are optimum values, but a reed with these values would play. The reed resonance frequency with these values ranged from 2600 to 3000 Hz. The force F results from the PAC and tube pressures, as well as the Bernoulli force acting on the reed. A value of 50 g/cm s was chosen for R as estimated from impulse excitations of an actual reed. An additional damping was added over a 5-mm interval on either side of the location of the teeth, to account for the damping of the lip. It should also be noted that A and K are both functions of position for a nonuniform bar, and this must be taken into account when developing the difference equation from the differential equation. The

force per unit length, F, is given by $F = (PT - PS)w - F_B$, where PT is the pressure in the tube mouthpiece, PS is the mouth (PAC) pressure, w is the reed width over which the pressure is applied, and F_B is the Bernoulli force per unit length given as

$$F_B = (\rho w/2)(U_R/A_R)^2. \tag{3}$$

Here, ρ is the air density, w is the width of the reed opening, U_R is the flow through the reed aperture, and A_R is the aperture area.

To solve the reed equation, an implicit numerical method described by Ames (1977) was used. The reed was divided into 1-mm sections, and the equation was solved for each section. In the method, the derivatives with respect to position at time t were written as the average of the derivatives at $t + \Delta t$ and $t - \Delta t$. Thus

$$\left(\frac{\partial^4 y}{\partial x^4}\right)_t = \frac{1}{2}\left[\left(\frac{\partial^4 y}{\partial x^4}\right)_{t+\Delta t} + \left(\frac{\partial^4 y}{\partial x^4}\right)_{t-\Delta t}\right]. \tag{4}$$

The boundary conditions which apply are $y = \partial y/\partial x = 0$ at the clamped end, and $\partial^2 y/\partial x^2 = \partial^3 y/\partial x3 = 0$ at the free end. Using the boundary conditions, the resulting equations can be written in a five-diagonal band matrix form, which was then solved using an IMSL routine (IMSL, 1982). More information, including the governing equations, concerning the reed model can be found in Appendix B.

In running the model, the force due to the teeth was applied at a distance of 8 mm from the tip of the reed. As the model ran, if a section of the reed collided with the mouthpiece, that section was held closed for as long as the reed tended to move into the mouthpiece. If the reed tip closed, the airflow through the mouthpiece was also set to zero. The resistance of the reed aperture was obtained by approximating the two wedge-shaped regions on the sides of the mouthpiece with rectangular sections, each section being 1 mm in length. The average opening of each section was used for the height of the rectangle, and the resistance of each rectangular section was added in parallel to the resistance of the other sections. The opening at the tip was also treated as a rectangular section, whose width was 1.3 cm, and whose height was equal to the reed opening at the tip. Van den Berg *et al.* (1957) gives the equation for the acoustic resistance of a rectangular slit:

$$R = 12\mu d /lw^3 + 0.875\rho U /2(lw)^2, \tag{5}$$

where l, w, and d are the length, height, and depth of the slit, and U is the volume velocity through the slit. The first term is due to viscosity, and the second term is due to kinetic effects. Thus the resistance of each section was calculated using Eq. (5), and the results were added in parallel.

The inductance of the reed aperture was determined using the equation $L = 2.85 \times 10^{-3} y_0^{-1/2}$, where y_0 is the opening at the tip of the reed. This equation was determined empirically by Stewart and Strong (1980) from the data given by Backus (1963), and fits his experimental data rather well.

The clarinet was represented in terms of its impulse response $h(t)$, obtained as the inverse Fourier transform of its input impedance. Frequency-dependent losses are incorporated in the clarinet input impedance and are mapped into the impulse response in the transform process. In the model,

the pressure in the tube (mouthpiece) is calculated as the convolution of the reed volume velocity with the impulse response. Typically, the impulse response is of rather long duration, and calculating the convolution sum can be somewhat costly. However, we opted to use the impulse response rather than the reflection function of Schumacher (1981) in spite of increased computational costs.

To obtain $h(t)$, one must know the input impedance of the instrument. For our study, we used a simplified clarinet consisting of a 415-mm length of cylindrical tube with an inner radius of 7.25 mm and with a clarinet mouthpiece attached. Seven tone holes, corresponding to the thumb hole and the six finger holes on an actual B-flat clarinet were placed along the tube. The positions of several of the holes were shifted slightly to simplify the numerical model, but the diameters of the tone holes correspond to those of an actual clarinet measured by Stubbins (1965). (The positions of the tone holes from the open end were 69, 93, 119, 174, 198, 229, and 248 mm.) Using this model of the clarinet, the input impedance was calculated using the method described by Plitnik and Strong (1979). The reed impedance was then added in parallel to the tube impedance. The impulse response was obtained via an inverse Fourier transform of the tube plus reed impedance. The impulse response was low-pass filtered with an 11-point Hanning window to eliminate computational, unphysical rapid fluctuations.

With the model in place on the computer, the simulation of the player–clarinet system was accomplished by sampling the system at 48 kHz. At each time interval, calculations were done, beginning at the lungs, to find the pressure in the player's mouth (PAC pressure), the pressure in the tube (mouthpiece), the airflow through the reed opening, and the area of the reed opening. Both waveforms and spectra could be obtained for the various quantities of interest.

II. EXPERIMENTAL RESULTS

An effort was made to obtain experimental values for the motion of the clarinet reed, since this could serve as a check on the reed model used in the numerical approach. Backus (1961) was able to obtain some results for the motion of the clarinet reed when it was excited in an artificial blowing chamber. We were able to extend his work and obtain pictures of the reed motion while it was being excited by an actual player. To measure the reed motion, a phototransistor was mounted on one side of the mouthpiece at the tip of the reed. An optical fiber was mounted on the opposite side of the mouthpiece, as shown in Fig. 2. The other end of the optical fiber was connected to a laser to provide a sufficiently intense light source for the phototransistor. As the reed vibrated, the amount of light reaching the phototransistor varied accordingly. Thus the output voltage of the phototransistor could be input to an oscilloscope, and the resulting trace mirrored the motion of the reed. Examples of the reed motion obtained for the written note C_4 at two levels are given in Fig. 3. (References to notes are to written notes; sounding notes would be two semitones lower.) These results and those for other notes are in good qualitative agreement with the results that Backus obtained by using an artificial blowing chamber.
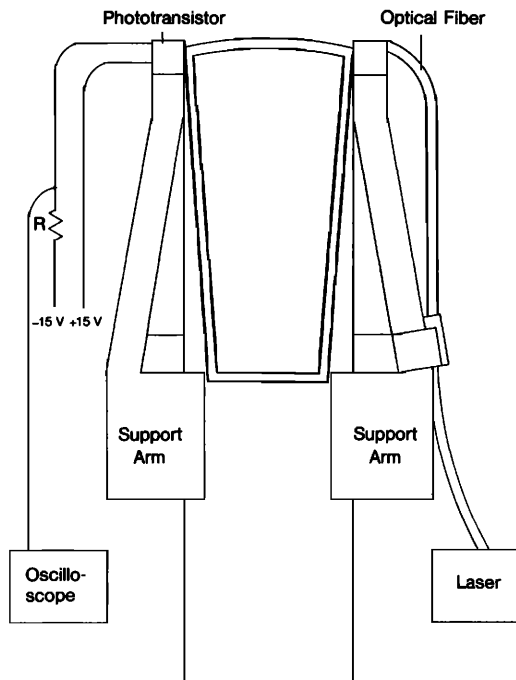

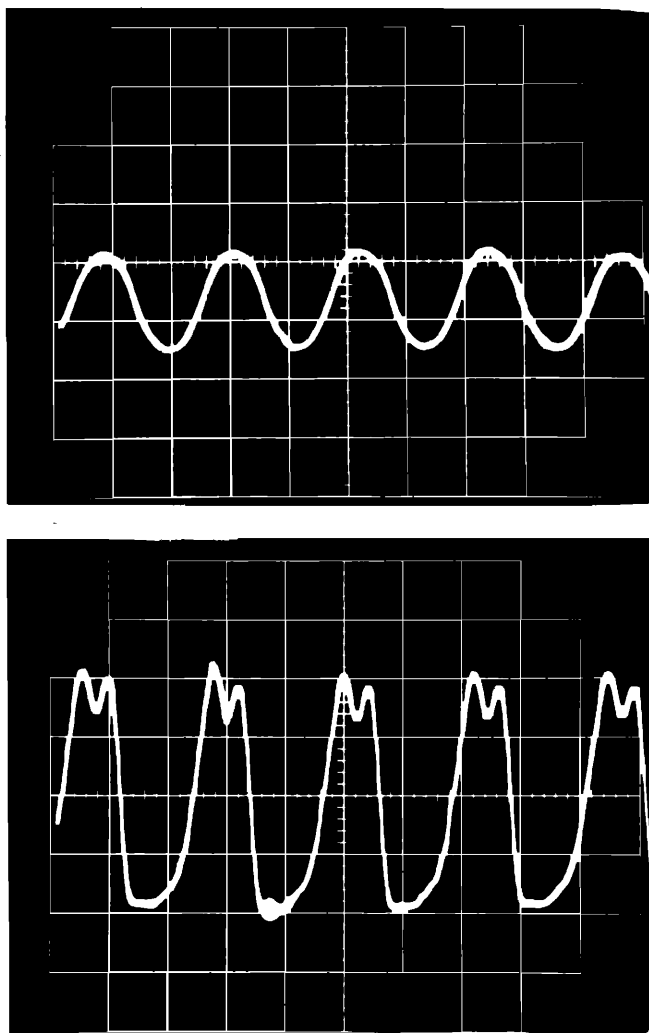FIG. 2. Apparatus for measuring the reed motion.

FIG. 3. Measured waveforms of the reed motion for the written note C_4: (upper) soft blowing; (lower) loud blowing.

III. NUMERICAL RESULTS

The calculated input impedance of the clarinet with three tone holes open for written C_4 is shown in Fig. 4. The cutoff frequency appears to lie beyond 1600 Hz. The effect of the reed (with natural frequency set to about 3000 Hz) in parallel with the tube is apparent in the small magnitude of the impedance near 3000 Hz. This figure is consistent with Figs. 1 and 2 from Thompson (1979) in which consideration was given to the role of the reed in clarinet tone production. One would expect large impedance peaks above 1600 Hz because of the "inadequacy" of the short tone hole lattice. Although not shown, these become apparent when the input impedance is examined above the reed frequency. They would be expected to "color" the corresponding impulse response.

The first 10 ms of the impulse response (obtained from the input impedance of Fig. 4) shown in Fig. 5 is more complex than similar impulse responses for some idealized clarinets in which the tapered mouthpiece is replaced with an equivalent volume of cylindrical tubing (see, for example, Fig. 6 in Schumacher, 1981). Part of the additional complexity is due to a negative wake trailing the initial impulse which is characteristic of tapered structures (Ayers *et al.*, 1985). A negative pulse returning from the first open tone hole about 2.3 ms after the initial pulse and a second negative pulse returning from the open end of the tube after about 3.0 ms are apparent in the figure. A positive pulse returns in about 4.6 ms after two round trips to the first open tone hole.

With the model, we first computed steady flow volume velocities as a function of reed rest opening. The "clarinet" was replaced by a resistive load equal to its characteristic impedance, and the subreed system was replaced by a constant pressure source. As a result, no oscillatory flow occurred. A number of different rest openings of the reed were specified and the flow computed as the pressure difference across the reed was changed. The results shown in Fig. 6 served as an aid in checking the reed and mouthpiece for proper behavior, as well as an aid in determining approximate threshold blowing pressures. The results exhibit the
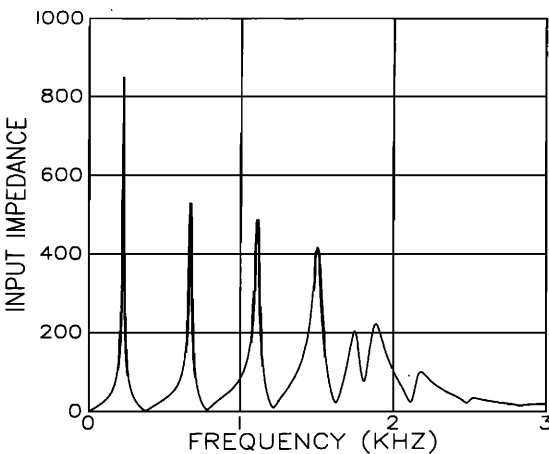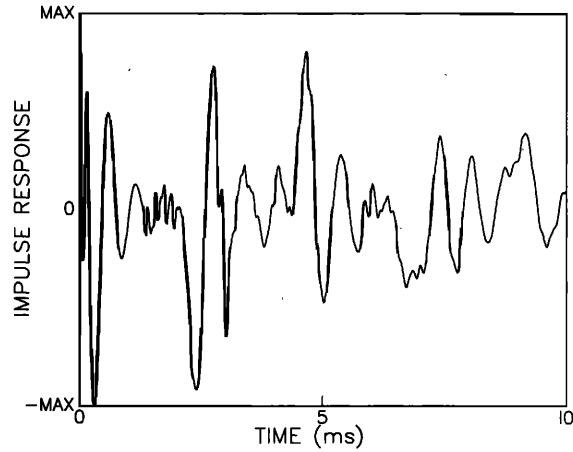

FIG. 5. Impulse response for clarinet with three tone holes open.

characteristics outlined by Benade (1976), and agree well with Stewart and Strong (1980). The flow increases initially as the pressure difference across the reed increases, but eventually a point is reached where the increased pressure difference begins closing off the reed and the flow decreases towards zero. The curves are asymmetrical, and the maxima occur at larger pressure differences for larger rest openings.

The model was also run to determine threshold blowing pressures. Again, a number of different rest openings were specified, and the blowing pressure was adjusted until the point was found where the model would just sustain oscillations. It should be pointed out that in obtaining the threshold pressures, a constant blowing pressure was used in place of the PAC system, in order to correspond as closely as possible to previous measurements made by others. The threshold blowing pressures so determined lie along the line shown in Fig. 7. For comparison, the results obtained by Backus (1963) are also shown by the triangles joined by a dotted line. Backus obtained his results as a function of average reed opening, rather than reed rest opening, as we have done. Thus, in preparing the figure, we have assumed that the average reed opening calculated by Backus is equal to half the

FIG. 4. Calculated input impedance of the clarinet with three tone holes open for the written note C_4. [Impedance is in units of acoustical ohms (cgs).]
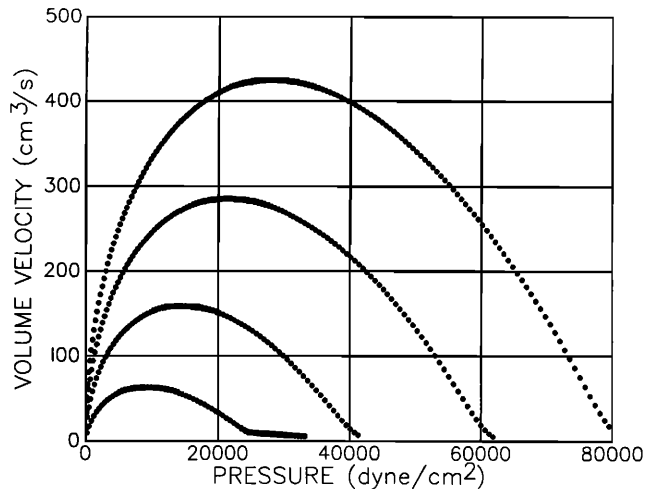

FIG. 6. Volume velocity in the clarinet model as a function of pressure difference across the reed for four different rest openings.
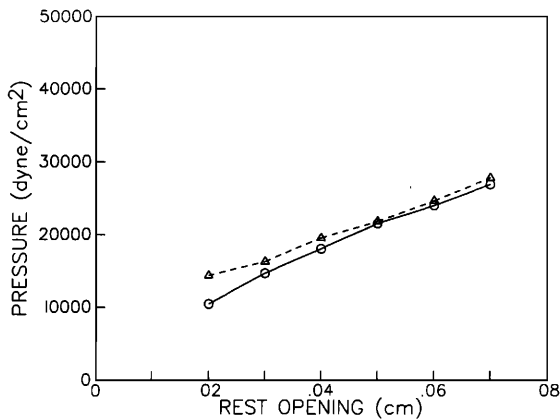
FIG. 7. Threshold blowing pressure for the clarinet model as a function of rest opening. The triangles joined by a dashed line show Backus' data.

FIG. 8. Cross-sectional area of the player's air column with an /ɑ/-shaped tract.

reed rest opening. It will be seen that the two curves agree reasonably well, particularly for larger rest openings. The discrepancies for smaller reed openings could result from a different reed stiffness or a different mouthpiece curvature lay between our model and the setup used by Backus.

In early simulation runs of the model, reed-opening waveforms having too many high-frequency components were obtained. We inadvertently discovered that the problem was made worse if the tube impulse response was scaled by a factor greater than 1. This led us to try scaling the impulse response by factors ranging from 0.4 to 0.8. We arbitrarily chose a scaling factor of 0.5 for the simulations because it gave reed-opening waveforms visually most similar to the experimental waveforms. There is some justification for this seemingly *ad hoc* procedure. Backus (1981) reported an anomalous behavior of a clarinetlike system which lowered the quality factor of the system by about a factor of 2 at amplitudes typical of playing conditions. Keefe (1983) discussed nonlinear losses that lower impedance peak heights relative to their small signal values that would be obtained in typical impedance measurements.

The model was run for several different notes using several vocal tract configurations to investigate any effect the PAC might have on the spectra of the clarinet. The vocal tract representations included: (1) constant blowing pressure, (2) /ɑ/-shaped tract, (3) /i/-shaped tract with a strong resonance at about 900 Hz, and (4) /i/-shaped tract with a stronger resonance at about 900 Hz. Cross-sectional areas of the PAC with an /ɑ/-shaped tract are shown in Fig. 8; those with the first /i/-shaped tract are shown in Fig. 9. The input impedance calculated for the PAC with an /ɑ/-shaped tract is shown in Fig. 10; that for the /i/-tract is shown in Fig. 11. The /ɑ/-tract PAC impedance has peaks of less than 50 Ω; the /i/-tract PAC impedance has a peak of about 170 Ω. The second /i/-tract PAC impedance had a peak of about 300 Ω. These values are consistent with Hoejke's (1986) measurements. Also, we investigated PAC impedance for 30 or so different vocal tract configurations. Only those PACs with /i/-like (or /ɪ/-like) vocal tract configurations produced impedance peaks of more than 100 Ω. The frequencies and amplitudes of the peaks could be shifted
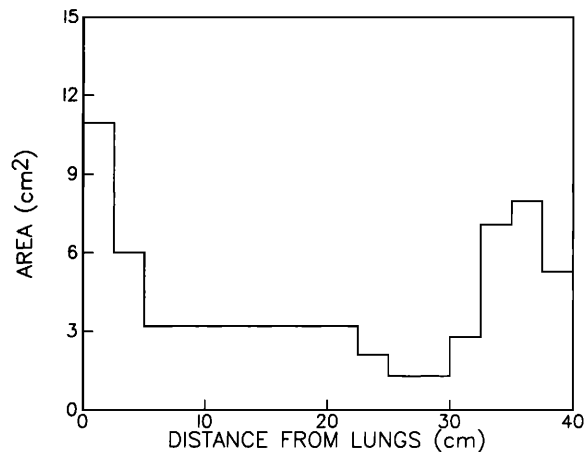
by altering the cross-sectional areas of the vocal tract sections.

Waveforms and spectra can be seen in Figs. 12–19 for different PAC and tube combinations. Except as otherwise noted, figures are for the written note C_4 on the clarinet, with a lung pressure of 34 000 dyn/cm^2 and a reed rest opening of 0.4 mm. Waveforms are shown for the reed opening, airflow through the reed aperture, mouth pressure, and tube (mouthpiece) pressure. The reed-opening and airflow spectra are shown relative to their respective dc values. Both pressure spectra are shown relative to the dc value of mouth pressure.

Waveforms for a constant mouth pressure of 33 000 dyn/cm^2 are shown in Fig. 12. There is quite good qualitative agreement between the reed waveforms obtained numerically (Fig. 12) and experimentally (Fig. 3). The reed is closed for about half of each cycle, as found experimentally for the beating reed case such as this. The reed opening waveform tends to mirror the tube pressure waveform as well, which is to be expected, since the reed is operating well below its resonance frequency, in its stiffness-controlled region. The reed opening spectrum shown in Fig. 13 exhibits a pre-
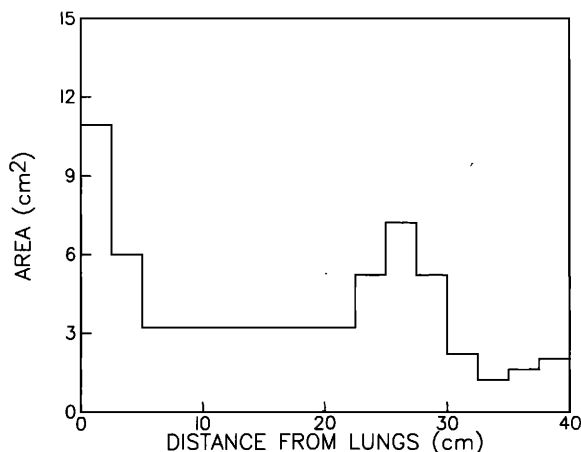

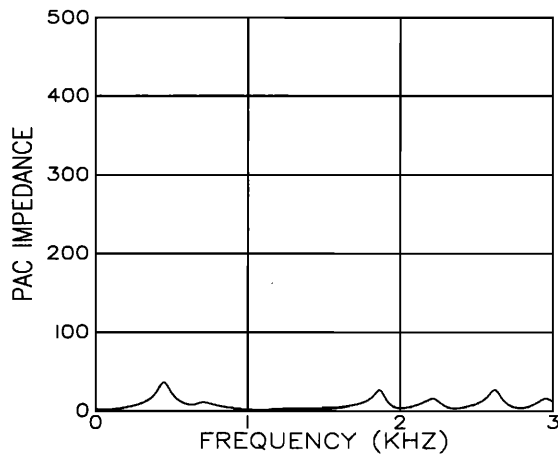FIG. 9. Cross-sectional area of the player's air column with an /i/-shaped tract.

FIG. 10. Input impedance of the player's air column with an /ɑ/-shaped tract.

FIG. 12. Calculated waveforms for the written note C_4 with a constant mouth pressure of 33 000 dyn/cm².

dominance of odd harmonics as would be expected for its approximately square-wave motion under the present simulation conditions. The airflow spectrum shown in Fig. 14 exhibits a nearly monotonic decrease of level with frequency. As expected, the spectrum of the constant mouth pressure (not shown) has no harmonic development. The tube pressure spectrum shown in Fig. 15 is consistent with combining the clarinet-impedance spectrum (Fig. 4) with the airflow spectrum (Fig. 14).

Waveforms for a PAC with an /ɑ/-shaped tract are shown in Fig. 16. The mouth pressure waveform is different from that of the constant mouth pressure case of Fig. 12, thus illustrating the effects of a pressure source with finite impedance. The other three waveforms are quite similar in the two cases. The mouth pressure spectrum shown in Fig. 17 exhibits some harmonic development but at levels more than 30 dB lower than the dc pressure. The other three spectra (not shown) are very similar to those of the constant pressure case.

Waveforms for a PAC with an /i/-shaped tract are shown in Fig. 18. With the exception of the mouth pressure waveform, these waveforms and their corresponding spectra
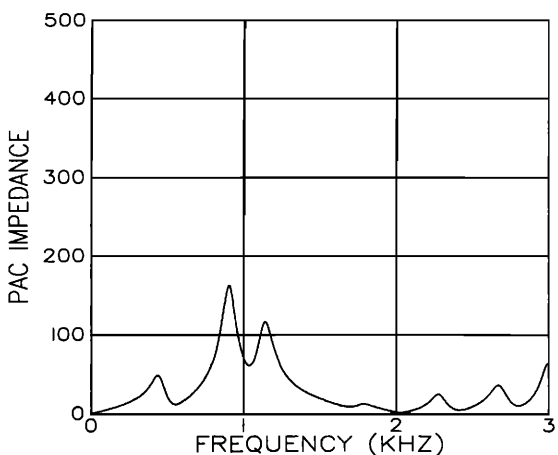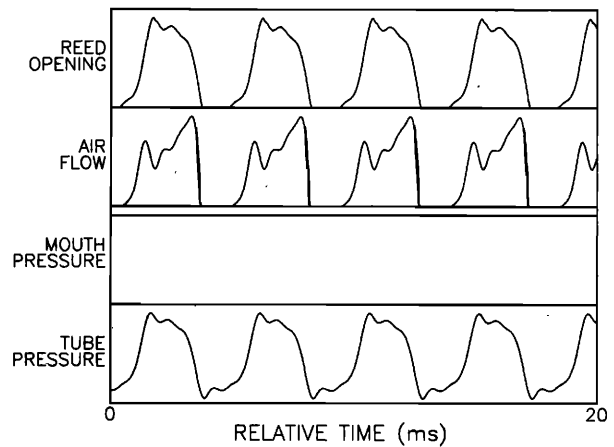
(not shown) are very similar to those for the /ɑ/ tract and constant mouth pressure cases. The mouth pressure spectrum for an /i/ tract shown in Fig. 19 exhibits a fourth harmonic at least 25 dB larger than that of the /ɑ/ tract in Fig. 17. (As noted previously, the pressure spectra are relative to the dc value of mouth pressure.)

This is due to the significant peak in the PAC impedance of Fig. 11 lying near the frequency of the fourth harmonic. These numerical results are consistent with experimental results of Benade (1983) and Hoekje (1986) in which a 40-dB mouth pressure level difference was found between the case of a "tuned" PAC and that of a "normal" PAC. They reported a 12-dB difference in tube pressure level for the two cases, whereas we observe essentially no change.

A striking case is shown in Fig. 20 in which a modified /i/-tract PAC with a larger amplitude resonance at about 900 Hz was used in conjunction with six tone holes open on the clarinet. In that case, the third partial predominates and takes over as the fundamental. This is the note one would obtain if the speaker key were opened. Presumably, the resonance of the PAC interacts to such an extent with the third harmonic (second mode of tube) in order to cause it to become the fundamental. After the simulation was run, this

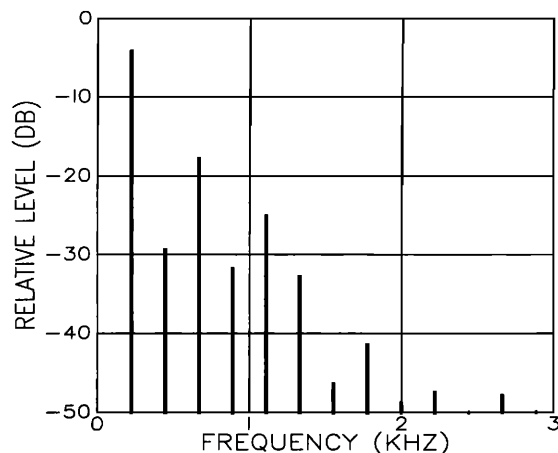FIG. 11. Input impedance of the player's air column with an /i/-shaped tract.

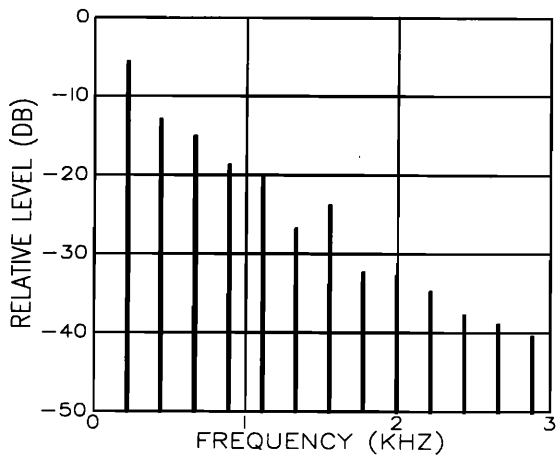FIG. 13. Reed opening spectrum for constant mouth pressure.

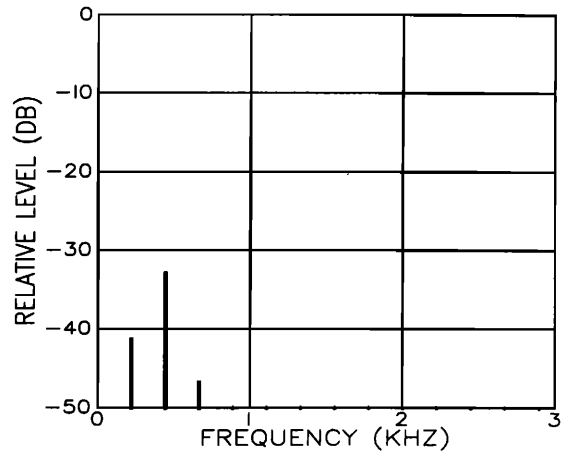FIG. 14. Airflow spectrum for constant mouth pressure.

FIG. 17. Mouth-pressure spectrum for a lung pressure of 34 000 dyn/cm² and an /ɑ/-shaped tract.
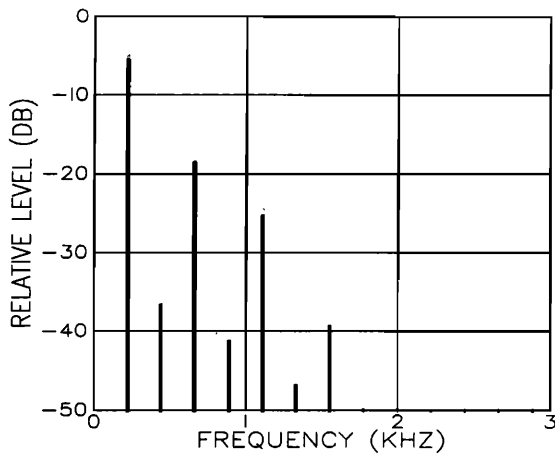

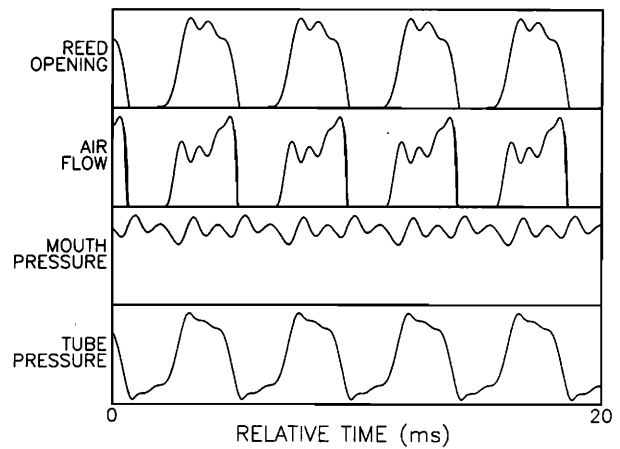FIG. 15. Tube-pressure spectrum for constant mouth pressure.

FIG. 18. Calculated waveforms for the written note C₄ with a lung pressure of 34 000 dyn/cm² and an /i/-shaped tract.
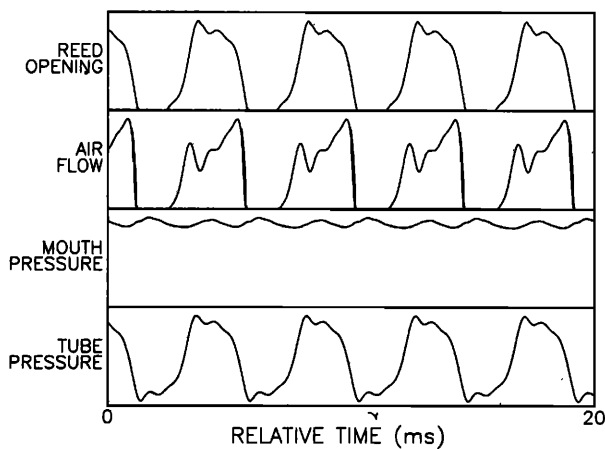

FIG. 16. Calculated waveforms for the written note C₄ with a lung pressure of 34 000 dyn/cm² and an /ɑ/-shaped tract.
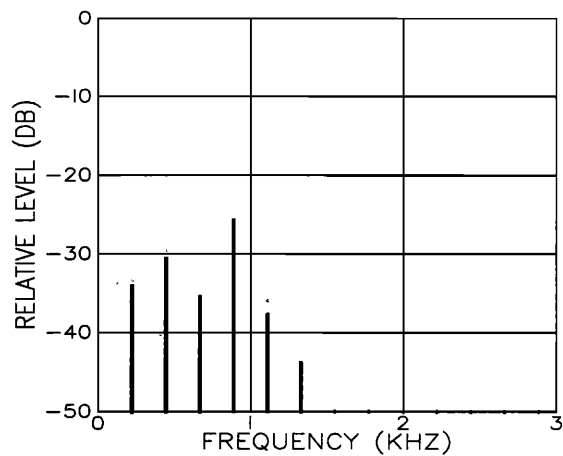

FIG. 19. Mouth-pressure spectrum for a lung pressure of 34 000 dyn/cm² and an /i/-shaped tract.
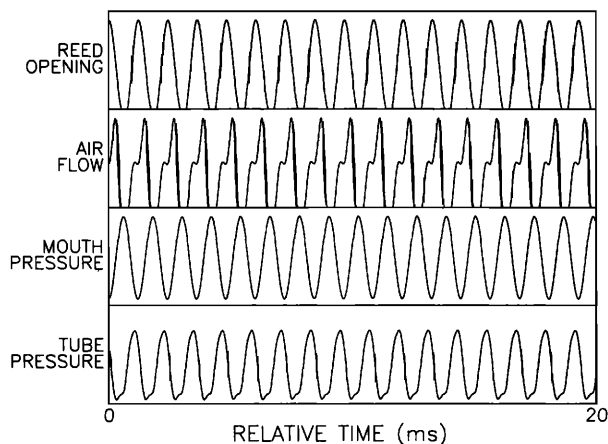
FIG. 20. Calculated waveforms for the written note C_4 with a lung pressure of 34 000 dyn/cm² and a modified /i/-shaped tract giving rise to a larger amplitude PAC peak than that of Fig. 11.

note was played on the actual simplified clarinet, and the third partial could be obtained as the fundamental when an /i/ tract was used. In the simulation, the /i/-tract PAC whose resonance was smaller in amplitude (Fig. 11) did not produce this effect.

Finally, in Fig. 21, we present an example of transient waveforms under conditions of constant mouth pressure. These show some features that are qualitatively similar to those shown in Fig. 35 of Hoekje (1986). However, the differences between parameter values in his experiment and our simulation are probably much greater for the transient case than for the steady-state cases.

With the exception of small differences, three of the waveforms in Figs. 12, 16, and 18 appear to be very similar. Note, however, that the oscillations in the PAC have a much larger amplitude with the /i/ tract than with the /ɑ/ tract. The fact that the mouth pressures are so dissimilar and the tube pressures so similar in Figs. 12, 16, and 18 is an indication that the reed decouples the clarinet from the PAC to a large extent.
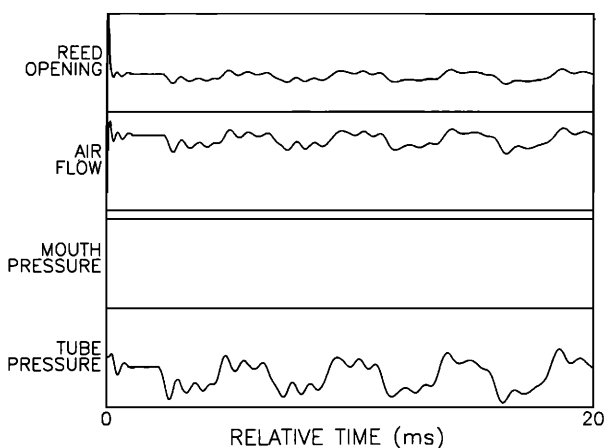

FIG. 21. Calculated initial transient waveforms for the written note C_4 with a constant mouth pressure of 33 000 dyn/cm².

IV. DISCUSSION

The main contribution of the research is the development of a "complete" player–clarinet model incorporating those aspects believed to be important in musical oscillations of a clarinet. The data presented may be regarded as representative of the mathematical problems involved; they may also be regarded as examples of clarinetlike systems of musical interest. The limitations of the musical value of the data are due, in part, to a clarinetlike structure that is not entirely faithful to an actual clarinet. Given the system studied, there were further limitations such as: (1) inadequate specification of the player's air column under study, including dimensions and tissue properties; (2) inadequate specification of tooth position and lip damping on the reed; (3) ad hoc amplitude normalization of the clarinet impulse response; (4) inadequate specification of lung pressure; and (5) too few experimental data with which to compare numerical data.

In spite of the foregoing limitations, we feel that the model developed shows considerable potential for the study of many of the issues dealing with the clarinet. It seems to behave rather well with respect to the threshold blowing pressure. The reed area waveform was similar to the experimental waveform. The waveforms and spectra seem quite realistic. Several experimentally observed phenomena, such as enhancement of the fourth harmonic in the mouth-pressure spectrum and the decoupling of spectra between mouth and tube, were generated in the simulation.

In the simulation, the vocal tract was demonstrated to be capable of influencing some spectra of the clarinet. Many of the data obtained show only subtle differences between different tract configurations, but some cases with more obvious differences were also found. An /i/-tract PAC appears capable of affecting particularly the partials in the region of 800–1100 Hz. This may well be part of the reason why many clarinet teachers teach their students to use an /i/ configuration in the higher register, and an /ɑ/ configuration in the lower register.

In the future, an effort should be made to obtain more appropriate parameters for the model and to employ them in various combinations. More experimental data from the actual system being modeled should be obtained with which to compare numerical results. It may be beneficial to add a speaker hole to the instrument to study the clarion register as there may be additional effects in that register which are not apparent in the chalumeau register studied.

ACKNOWLEDGMENTS

APPENDIX A: PLAYER'S AIR COLUMN MODEL

The player's air column was treated as an analogous electric circuit, as shown in Fig. 1. The differential equations which describe the system are:

$$P_I - U_1(t)(R_I + R_1) - L_1 \frac{dU_1(t)}{dt}$$

$$-\frac{1}{C_1} \int \left[(U_1(t) - UG_1(t) \right] dt = 0,$$

$$\frac{1}{C_1} \int \left[UG_1(t) - U_1(t) \right] dt$$

$$+ (1/G_1) \left[UG_1(t) - UA_1(t) \right] = 0,$$

$$(1/G_1) \left[UA_1(t) - UG_1(t) \right] + B_1 \left[UA_1(t) - U_2(t) \right]$$

$$+ \frac{1}{K_1} \int \left[UA_1(t) - U_2(t) \right] dt$$

$$+ M_1 \left(\frac{dU A_1(t)}{dt} - \frac{dU_2(t)}{dt} \right) = 0,$$

$$P_1(t) - U_2(t)(R_1 + R_2) - (L_1 + L_2) \frac{dU_2(t)}{dt}$$

$$-\frac{1}{C_1} \int \left[U_2(t) - UG_2(t) \right] dt = 0,$$

$$\vdots$$

$$P_N(t) - U_R(t)(R_N + R_R(t))$$

$$- \left[L_N + L_R(t) \right] \frac{dU_R(t)}{dt} - PT(t) = 0,$$

where

$$R_n = S_n l_n (\pi \rho \mu f)^{1/2} / 2A_n^2,$$

$$L_n = \rho l_n / 2A_n,$$

$$C_n = A_n l_n / \rho c^2,$$

$$G_n = \left[S_n (\eta - 1) l_n / \rho c^2 \right] \sqrt{\lambda \pi f / c_p \rho},$$

P_I = lung pressure,

l_n = length of nth section,

S_n = circumference of nth section,

A_n = area of nth section,

c = 35 000 cm/s,

μ = 0.000186 dyn s/cm$^2 \equiv$ viscosity of air,

ρ = 0.00114 g/cm$^3 \equiv$ density of air,

f = frequency,

$\lambda = 0.055 \times 10^{-3}$ cal/cm s deg $\equiv$ coefficient of heat conduction,

c_p = 0.24 cal/g deg $\equiv$ specific heat of air,

η = 1.4 $\equiv$ adiabatic constant,

$U_n(t)$ = volume velocity of nth section,

$UG_n(t)$ = volume velocity of nth loop containing compliance (C_n) *and* conductance (G_n),

$UA_n(t)$ = volume velocity of nth loop containing conductance (G_n) *and* wall admittance ($B_n M_n K_n$),

$R_R(t)$ = reed aperture resistance,

$L_R(t)$ = reed aperture inductance,

$PT(t)$ = pressure in mouthpiece, as described in the text.

The yielding walls of the player's air column were modeled as a lumped element mass-compliance-viscous (MKB) circuit. Average values for B, M, and K were obtained from Ishizaka *et al.* (1975). The values chosen for this study were: B = 900 g/s, M = 1.8 g, and K = 150 000 dyn/cm. In solving the equations, the integrals were represented as sums, and the derivatives as first-order, backward difference equations.

APPENDIX B: MODEL OF THE REED

We repeat Eq. (2) which is used to determine the reed motion:

$$\rho A \frac{\partial^2 y}{\partial t^2} + R \frac{\partial y}{\partial t} = -\frac{\partial^2}{\partial x^2} \left(YAK^2 \frac{\partial^2 y}{\partial x^2} \right) + F.$$

If we let the area A be written as $wb(x)$, where w is the width of the reed and $b(x)$ is the thickness of the reed at position x, and K^2 be written as $b^2(x)/12$, then the equation can be written as

$$\rho wb(x) \frac{\partial y^2}{\partial t^2} + R \frac{\partial y}{\partial t} = -\frac{1}{12} Yw \frac{\partial^2}{\partial x^2} \left(b^3(x) \frac{\partial^2 y}{\partial x^2} \right) + F.$$

For first derivatives, we use the central difference formula: $\partial y / \partial x \approx (y_{i+1} - y_{i-1})/2\Delta x$. For second derivatives, we use the central difference formula: $\partial^2 y / \partial x^2 \approx (y_{i-1} - 2y_i + y_{i+1})/(\Delta x)^2$. Thus the term on the right-hand side of the equation becomes

$$\frac{\partial^2}{\partial x^2} \left(b^3 \frac{\partial^2 y}{\partial x^2} \right) \approx \frac{(y_{i-2,j} - 2y_{i-1,j} + y_{i,j})b_{i-1}^3}{(\Delta x)^4}$$

$$-\frac{2(y_{i-1,j} - 2y_{i,j} + y_{i+1,j})b_i^3}{(\Delta x)^4}$$

$$+\frac{(y_{i,j} - 2y_{i+1,j} + y_{i+2,j})b_{i+1}^3}{(\Delta x)^4},$$

where the second index on y refers to time. For the x derivatives at time $t = t_j$, the average of the values at $t = t_{j-1}$ and $t = t_{j+1}$ is used. If we define constant λ as $\lambda = Yw(\Delta t)^2 / 24(\Delta x)^4$, then the difference equation can be written as

$$\lambda b_{i-1}^3 y_{i-2,j+1} - 2\lambda (b_{i-1}^3 + b_i^3) y_{i-1,j+1} + \left[\rho wb_i + \tfrac{1}{2}R\Delta t + \lambda (b_{i-1}^3 + 4b_i^3 + b_{i+1}^3) \right] y_{i,j+1}$$

$$- 2\lambda (b_i^3 + b_{i+1}^3) y_{i+1,j+1} + \lambda b_{i+1}^3 y_{i+2,j+1} = 2\rho wb_i y_{i,j} - \lambda b_{i-1}^3 y_{i-2,j-1} + 2\lambda (b_{i-1}^3 + b_i^3) y_{i-1,j-1}$$

$$+ \left[\tfrac{1}{2}R\Delta t - \rho wb_i - \lambda (b_{i+1}^3 + 4b_i^3 + b_{i-1}^3) \right] y_{i,j-1}$$

$$+ 2\lambda (b_i^3 + b_{i+1}^3) y_{i+1,j-1} - \lambda b_{i+1}^3 y_{i+2,j-1} + F(\Delta t)^2.$$

The boundary conditions that the reed must satisfy are $y = \partial y / \partial x = 0$ at $x = 0$, and $\partial^2 y / \partial x^2 = \partial^3 y / \partial x^3 = 0$ at the tip of the reed. If there are N sections for the reed, with the Nth section being the tip of the reed, the difference equations that satisfy the boundary conditions are

$$y_{0,j} = 0 \quad (y = 0 \text{ at } x = 0),$$

$$y_{-1,j} = y_{1,j} \quad \left(\frac{\partial y}{\partial x} = 0 \text{ at } x = 0\right),$$

$$y_{N+1,j} = 2y_{N,j} - y_{N-1,j},$$

$$y_{N+2,j} = y_{N,j} - 4y_{N-1,j} + y_{N-2,j}$$

$$\left(\frac{\partial^2 y}{\partial x^2} = \frac{\partial^3 y}{\partial x^3} = 0 \text{ at } x = x_N\right).$$

The above equations can be written as a system of simultaneous equations that can be solved implicitly. The resulting coefficient matrix is a five-diagonal band matrix, which was solved using the IMSL routine LEQT2B (IMSL, 1982).

The values chosen to run the model were as follows: $Y = 6 \times 10^{10}$ dyn/cm^2, $\rho = 0.5$ g/cm^3, $w = 1.3$ cm, $R = 50$ g/cm s, $\Delta t = 1/48\,000$ s, and $\Delta x = 1$ mm. The values for $b(x)$ can be obtained by measuring a clarinet reed. For the region of interest, the function $b(x) = 0.081 - 0.047x$ was found to match the measurements of an actual reed rather well, so this function was used to determine the reed thickness. The value of R can be obtained by running the reed model separately. If the reed is excited by an impulse, the reed will oscillate with an exponentially decaying amplitude. The value of R determines how quickly the amplitude decays, and R can be varied until the decay matches the decay that can be observed experimentally by exciting the reed with an impulse force.

When the model was functioning, the location where the teeth apply a force on the reed, and the magnitude of the applied force were specified. This determined the initial rest opening between the reed and the mouthpiece. The rest opening between the reed and the mouthpiece with no force applied was given by $0.04667x^2$, where x is the distance along the lay, or curved part of the mouthpiece. The lay was taken to be 15 mm in length. This corresponds to a mouthpiece with a medium-short lay and a medium-open tip opening. Also, additional damping was added to the reed for 5 mm on either side of the location of the teeth to account for the damping of the lip in contact with the reed.

Allen, D. R., and Strong, W. J. (1985). "A model for the synthesis of natural sounding vowels," J. Acoust. Soc. Am. 78, 58–69.

Ames, W. F. (1977). Numerical Methods for Partial Differential Equations, (Academic, New York), 2nd ed., pp. 279–281.

Ayers, R. D., Eliason, L. J., and Mahgerefteh, D. (1985). "The conical bore in musical acoustics," Am. J. Phys. 53, 528–537.

Backus, J. (1961). "Vibrations of the reed and the air column in the clarinet," J. Acoust. Soc. Am. 33, 806–809.

Backus, J. (1963). "Small-vibration theory of the clarinet," J. Acoust. Soc. Am. 35, 305–313.

Backus, J. (1981). "Anomalous behavior of a clarinetlike system," J. Acoust. Soc. Am. Suppl. 1 70, S23.

Backus, J. (1985). "The effect of the player's vocal tract on woodwind instrument tone," J. Acoust. Soc. Am. 78, 17–20.

Benade, A. H. (1976). Fundamentals of Musical Acoustics (Oxford University, New York).

Benade, A. H. (1983). "Air column, reed, and player's windway interaction in musical instruments," in Vocal Fold Physiology, edited by I. R. Titze and R. C. Scherer (The Denver Center for the Performing Arts, Denver, CO), pp. 425–452.

Benade, A. H., and Gans, D. J. (1968). "Sound production in wind instruments," Ann. N. Y. Acad. Sci. 155, 247–263.

Benade, A. H., and Hoekje, P. L. (1982). "Vocal tract effects in wind instruments," J. Acoust. Soc. Am. Suppl. 1 71, S91.

Clinch, P. G., Troup, G. J., and Harris, L. (1982). "The importance of vocal tract resonance in clarinet and saxophone performance, a preliminary account," Acustica 50, 280–284.

Flanagan, J. L. (1972). Speech Analysis Synthesis and Perception (Springer, New York), 2nd ed., pp. 25–35.

Hoekje, P. L. (1986). "Intercomponent energy exchange and upstream/downstream symmetry in nonlinear self-sustained oscillations of reed instruments," Ph.D. dissertation, Case Western Reserve University, Cleveland, OH.

IMSL Library (1982). IMSL Marketing Services Division, 2500 Park West Tower One, 2500 City West Boulevard, Houston, TX 77042.

Ishizaka, K., French, J. C., and Flanagan, J. L. (1975). "Direct determination of vocal tract wall impedance," IEEE Trans. Acoust. Speech Signal Process. ASSP-23, 370–373.

Ishizaka, K., Matsudira, M., and Kaneko, K. (1976). "Input acoustic-impedance measurement of the subglottal system," J. Acoust. Soc. Am. 60, 190–197.

Keefe, D. H. (1983). "Acoustic streaming, dimensional analysis of nonlinearities, and tone hole mutual interactions in woodwinds," J. Acoust. Soc. Am. 73, 1804–1820.

Kinsler, L. E., Frey, A. R., Coppens, A. B., and Sanders, J. V. (1982). Fundamentals of Acoustics, (Wiley, New York), 3rd ed., pp. 68–75.

McIntyre, M. E., Schumacher, R. T., and Woodhouse, J. (1983). "On the oscillations of musical instruments," J. Acoust. Soc. Am. 74, 1325–1345.

Mooney, J. E. (1968). "The effect of the oral cavity on the tone quality of the clarinet," Ph.D. dissertation, Brigham Young University, Provo, UT.

Plitnik, G. R., and Strong, W. J. (1979). "Numerical method for calculating input impedances of the oboe," J. Acoust. Soc. Am. 65, 816–825.

Schumacher, R. T. (1978). "Self-sustained oscillations of the clarinet: an integral equation approach," Acustica 40, 298–309.

Schumacher, R. T. (1981). "Ab initio calculations of the oscillations of a clarinet," Acustica 48, 71–85.

Sommerfeldt, S. D. (1986). "Simulation of a player–clarinet system," M. S. thesis, Brigham Young University, Provo, UT.

Stewart, S. E. and Strong, W. J. (1980). "Functional model of a simplified clarinet," J. Acoust. Soc. Am. 68, 109–120.

Strong, W. J., and Sommerfeldt, S. D. (1986). "Simulation of flow through a parameterized 'reed-aperture'," 12th International Congress on Acoustics, Toronto, July 1986.

Stubbins, W. H. (1965). The Art of Clarinetistry (Ann Arbor, Ann Arbor, MI).

Thompson, S. C. (1979). "The effect of the reed resonance on woodwind tone production," J. Acoust. Soc. Am. 66, 1299–1307.

Titze, I. R. (1984). "Parametrization of the glottal area, glottal flow, and vocal fold contact areas," J. Acoust. Soc. Am. 75, 570–580.

Van den Berg, Jw., Zantema, J. T., and Doorneball, P. (1957). "On the air resistance and the Bernoulli effect of the human larynx," J. Acoust. Soc. Am. 29, 626–631.

Worman, W. E. (1971). "Self-sustained nonlinear oscillations of medium amplitude in clarinet-like systems," Ph.D. dissertation, Case Western Reserve University, Cleveland, OH.